Petroleum and Coal

Article **Open Access**

Pore Pressure Prediction and Fracture Pressure Estimation using Well Logs and Seismic Data from Cobalt Field, Offshore Niger Delta

Mpara Carine Bonkga [1], Olugbenga A. Ehinola [1,3], Kennedy F. Fozao [2], Yinka A. Olayinka [3], Olutayo Y. Lawal [3], and Oladotun A. Oluwajana [1,4]*

[1] *Pan African University of Life and Earth sciences, Department of Geology, University of Ibadan, Ibadan, Nigeria*
[2] *Department of Petroleum Engineering, NAHPI-School of Engineering, University of Bamenda, Cameroon*
[3] *Energy and Environmental Research Group, Department of Geology, University of Ibadan, Ibadan, Nigeria*
[4] *Department of Earth Sciences, Adekunle Ajasin University, Akungba-Akoko, Nigeria.*

Received January 17, 2022; Accepted June 14, 2022

Abstract

The work is aimed at predicting shale pore pressures in order to identify the different pressure zones and estimate fracture pressures in some wells in COBALT Field, Niger Delta. To achieve this, geoscientific software was used to analyze the well log data. The data was quality checked and true vertical depth computation was carried out to facilitate overburden stress estimation. The extrapolation method was used to compute the overburden stress, through the merging of the bulk density log and the synthetic bulk density that was generated. Using a gamma ray log, mechanical stratigraphy for lithology delineation was carried out to delineate shales from sands. Normal compaction trendline was applied to sonic and resistivity logs using Eaton's method together with Bower's sonic method to predict pore pressures. The Mathews and Kelly's empirical method was applied to vertical stress and pore pressures obtained to estimate fracture pressures. Also, Petrel software was used for seismic interpretation, after which time and depth maps were generated. The tops of overpressure ells were incorporated into structural maps to show the distribution of the tops of overpressure wells. It was observed that Wells Cobalt- 01 and 06 are normal pressure wells with the highest-pressure values of 8.61 and 8.67 ppg, respectively; while Wells Cobalt-02, 03, 04, and 05 were over-pressured with values of 10.9, 9.5, 10.5, and 10.01 ppg respectively, with corresponding depths of 1288, 12057, 9674, and 1019 FTTVD, respectively. The fracture pressure for each well was also estimated from the pore pressures. The main mechanisms responsible for overpressure in the COBALT field were identified as loading and unloading, with a small contribution from fault-related lateral pressure transfer. The results observed from the depth map show that the top of overpressure wells is distributed or compartmentalized into different fault blocks. The outcome of this work could facilitate proper planning and drilling of future wells in the field.

Keywords: *Pore pressure; Fracture pressure; Overburden stress; Normal compaction trendline; Eaton's method.*

1. Introduction

Pore pressure is the pressure acting on fluids within the pores of a reservoir [1]. Pore pressure is also referred to as formation pressure. Technology has facilitated a lot of things and made it easier to achieve various ways of acquiring information on pore pressure before embarking on a journey of petroleum activities such as drilling and production, predicting any sudden expectations and looking for ways to overcome such challenges either at high-or low-pressure zones. Incomplete knowledge and information about Formation pressure while engaging in drilling activities has led to a lot of devastating situations such as loss of lives,

equipment, and uncontrollable flow of oil onto the surface. If high-pressure zones are accurately predicted and detected, many accidents will be avoided and drilling time will be reduced. Predicting the pore pressure of reservoirs in a field is a major component of exploration, exploitation, and development risk analysis [2-3]. Knowledge of Formation pressure is very important in the development of oil and gas fields. Petroleum geologists' ability to determine likely traps, seals, and map hydrocarbon pathways by accessing trap design and basin modelling is dependent on their understanding of reservoir pore pressure [4-8].

Also, formation pressure prediction or pore pressure prediction is critical and very necessary because it facilitates decision-making in well planning and operations, safety conditions for personnel in charge, as well as equipment in use. The outcome from pore pressure prediction determines casing design and drilling fluid to be used during drilling. Without information and knowledge on pore pressure, certain problems are likely to occur, such as kicks, influx, and blowouts. On the other hand, if this information is available, pre-preparations and better planning will be done to overcome such challenges.

1.1. Previous studies

Pore pressure prediction using shale parameters acquired from well log data was first investigated by [9]. They calculated overpressures by plotting acoustic velocity and resistivity data from shale in Texas and Louisiana, USA. They showed that resistivity had a normal trend with depth while sonic wave travel time gave a logarithmic relationship with depth in the normally pressured interval. According to [10-12], this pressure-depth relationship measured with a sonic and resistivity log is known as the normal compaction trend (NCT). Any deviation in measured parameters from the usual trendline was used in this approach. Many researchers have successfully predicted pore pressure using resistivity, sonic transit time porosity, and other well log data. Pore pressure research is mostly predicated on the concept that any change in normal pressure causes changes in petrophysical parameters like compaction, porosity, and fluid motion. This indicates that observable metrics that can demonstrate these changes can be used to interpret and quantify pore pressure [13]. The pore pressure and the fracture gradient define the mud weight that is required during drilling. Whereas [14] provided an equation that accounted for overburden stress and hydrostatic pressure in his work to predict pore pressure using a normal compaction trend line and observed acoustic sonic wave travel time. This equation also uses resistivity data, and this takes into consideration a single NCT for the entire depth of the well and assumes one overpressure origin, which is disequilibrium compaction or undercompaction, but most times empirically modified to account for multiple mechanisms.

Bowers presented a method different from Eaton that considers disequilibrium compaction and an unloading effect that results from fluid expansion [15]. He showed that a drop in sonic velocity without a decrease in bulk density could come from an unloading effect. He carried out this work in many Formations using data from the Gulf of Mexico and derived effective stress from pore pressure and overburden stress based on sonic log data.

Both Eaton and Bowers [14] and [15] methods are based on the fact that porosity decreases with burial depth in a normally pressured Formation or hydrostatically pressured Formations. Also, areas with overpressure usually reduce the tendency for porous rocks to compact, leaving them with high porosity. Swarbrick conducted his research and provided some porosity method lobe holes [16].

A lot of challenges are faced in the petroleum industry, such as increased nonproductive time, stock pipe, formation fracture, wellbore instability, kicks, blowouts, loss of lives, and damaged equipment. This is made worse because accurate information is not readily available to petroleum drilling companies. Again, most problems also arise from the drilling fluid in which mud weights are not accurately designed and also from the fact that casing designs do not match the required depth or are not properly selected. Furthermore, most challenges are not well managed due to inadequate risk preparation and poor incident response. Also, inadequate monitoring or attention, which sometimes results from the staff. Lastly, even though

unavailability of data is often the problem, most of the time data is not available to do the necessary checks required before embarking on an activity such as drilling.

In the report titled Loss of well control occurrence and size estimation by [17], his report showed that between 2000-2015, 45% of Loss Of Well Control (LOWC) reported in the SINTEF Offshore blowout events occurred during drilling. And Nigeria recorded 2 exploration drilling blowout events. This means that this problem is not just Nigeria's but a worldwide problem. Therefore, this study will therefore provide the pressure distribution in this field "COBALT" and the cause of the pressure, which will aid with information that would be of importance to the drilling and production industry.

The aims and objectives of this study are to predict pore pressure and identify geopressured zones from well logging and seismic data. That is to identify normal, subnormal, abnormal, and overpressure zones. Also, an estimation of pore and fracture pressures were made to determine the influence of pore and fracture pressure on wellbore stability and production of maps for the top of overpressure wells to observe the effect of faults.

1.2. Geological setting

The Cobalt field is found in the offshore portion of the Niger Delta Basin (Figure 1). The Niger Delta is a prolific basin that is ranked among the topmost producing basins in the world and Africa at large. It is found at the apex of the Gulf of Guinea on the West African continent [18], which is part of the triple junction formed in the Cretaceous during the continental breakup.

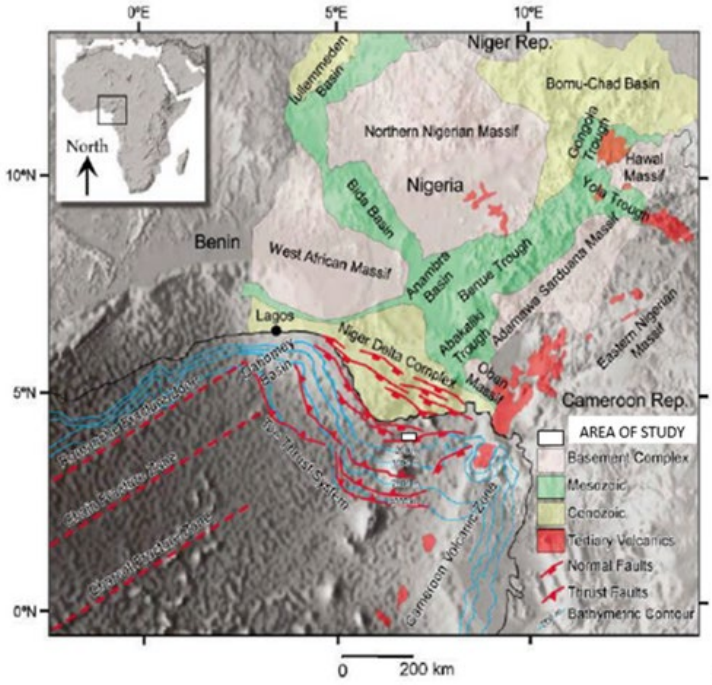

Figure 1. Location and distribution of wells in study area

The Niger Delta Basin is bounded in the west by the Dahomey basin, in the east by the Cameroun volcanic line/Abakaliki fold belt, in the north by the Anambra Basin, and in the south by the Gulf of Guinea 4000m bathymetric contour. It is situated in the southern part of Nigeria, between longitudes 3–90E and latitudes 4–60N. It is made up of depobelts that form one of the largest regressive sequences in the world and a highly prolific hydrocarbon province delta with an area of about 300,000 km^2 [18-19]. According to [20] Hospers 1965, the Niger Delta is comprised of 500,000 km^3 of sediments, covers an area of 75000 km2 and consists of a 12 km thick sedimentary structure that indicates a progradational package [18-19,21-22]. A lot of studies have been carried out by many researchers concerning the evolution and stratigraphy of this basin.

The geodynamics of the separation of the African and South American continents, as well as the tectonics of the development of the Benue Trough during the Late Jurassic, are intimately tied to the evolution of the Niger Delta.

2. Materials and methods

The following datasets were used: The dataset for this project was provided by a petroleum company in Nigeria. The datasets provided were well logs for six wells (Cobalt 1 to 6), deviations, checkshots for all six wells, and 3D seismic data in the Cobalt Field. Figure 2 shows the

workflow adopted to achieve the objectives of this study. The methodology adopted to realize the objectives of this work is described in Figure 2 and explained as follows.

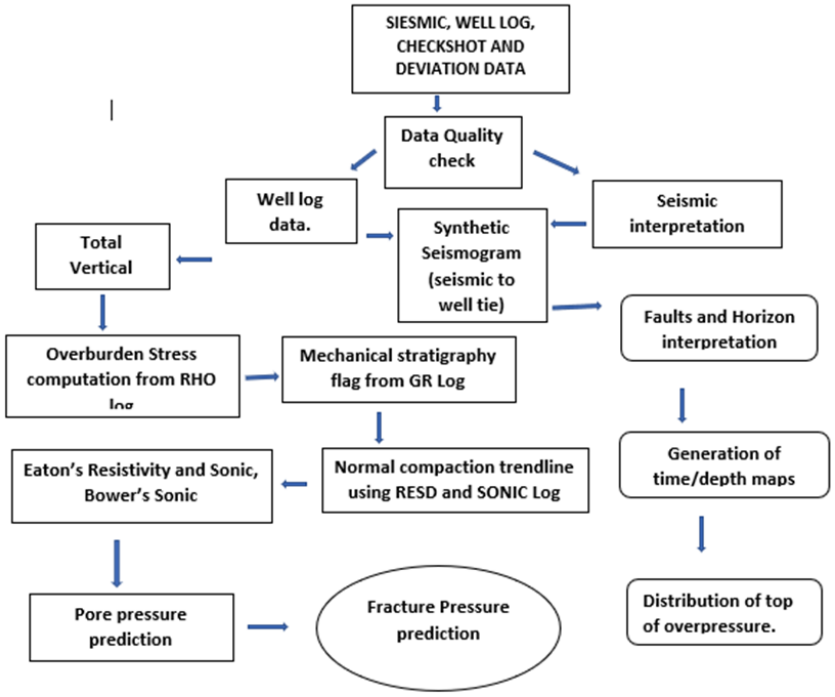

Figure. 2. Workflow adopted to achieve the objectives of this study

2.1. True vertical depth (TVD) computation

The TVD computation is essential for conversion from measured depth (MD) to TVD since the overburden stress needs to be calculated for the entire depth. This conversion was done for each well. TVD computations are important in the determination of bottom hole pressures, which are caused partly by the hydrostatic head of fluid in the wellbore.

2.2. Overburden stress or lithostatic pressure

The extrapolation method was used in this work to calculate overburden stress. The density profile was built at depth with the logged bulk density, then the composite or synthetic bulk density was built using the assumed salt density and densities of the formation. Seawater density is considered at 1.03g/cm3, which is essential for the overburden stress calculation. Therefore, by integrating this synthetic density with logged bulk density, overburden stress (equation 1) and overburden gradient were obtained.

$$S = \rho_f gz \ldots\ldots\ldots\ldots \quad (1)$$

where z, ρ_f and g are the height of the column, the fluid density, and acceleration due to gravity, respectively.

2.3. Mechanical stratigraphy and well correlation

The mechanical stratigraphy flag is done by using gamma Ray for lithology discrimination to delineate between sands and shales. The Gamma Ray index (GRI) was used to calculate the volume of shale (equation (2)). The Gammar Ray measures the natural radioactivity in the formation and it is this property which helps to identify the lithologies.

$$IGR = \frac{GRlog - GRmin}{(GRmax - GRmin)} \ldots \quad (2)$$

where: IGR = Gamma ray index ;GRlog = Gamma ray estimation from the GR log in the zone of interest ;GRmin = Minimum gamma ray for the clean sand ;GRmax = Maximum gamma ray for the shale.

2.4. Pore pressure prediction

The Eaton Resistivity and Bowers method were used because the Niger Delta is a Tertiary Basin and the main processes that lead to the generation of overpressure in these Tertiary Basins (Gulf of Mexico, Niger Delta) are rapid deposition, subsidence, and burial in low permeable sediments [23-25] such as shales, causing mechanical disequilibrium compaction, which is a function of effective stress.

2.4.1. Eaton's sonic velocity method with depth-dependent normal compaction trendline

Pore pressure gradient prediction from sonic compressional transit time (Δtn) was achieved based on [14] Eaton's (1975) empirical equation (equation 3).

$$Ppg = \mathrm{OBG} - (\mathrm{OBG} - \mathrm{Ph})\left(\frac{\Delta \mathrm{tn}}{\Delta \mathrm{t}}\right)^{m} \ldots \quad (3)$$

where Δt is the transit time in shales obtained from the well log; Δtn is the transit time in shales at the normal pressure; Ph is hydrostatic pressure; OBG is the overburden stress; m is an exponent, and normally the exponent; m = 3 can be applied in case the overpressure was generated by undercompaction without any secondary mechanism of pore pressure generation.

The transit time (Δtn) is determined from the normal compaction trendline in normal pressure conditions, and it is obtained by applying in Eaton's sonic method.

2.4.2. Eaton's resistivity method with depth dependent normal compaction trendline

The same equation (Eaton's equation) was used, and the same input parameters were applied except that sonic wave travel time was replaced by resistivity log as shown in equation (4)

$$PPg = \mathrm{OBG} - (\mathrm{OBG} - \mathrm{PPN})\left(\frac{R}{R_N}\right)^{x} \ldots \quad (4)$$

where 'PPg' is the pore pressure gradient (ppg); 'OBG' is the Overburden gradient (ppg); 'PPN' is regarded as the normal pore pressure gradient (ppg); "R" is the observed resistivity (ohms-m); "R_N" is the Normal Resistivity (ohms-m); and "x" is the Eaton exponent, which is 1.2 and the Eaton Resistivity exponent of 1.

In Eaton's equation, there is always a problem in determining the shale resistivity at hydrostatic pore pressure. This calls for the need for a compaction trendline for pore pressure prediction. Rn, which is the normal resistivity function of burial depth, can be calculated from the normal compaction trend line using equation 5.

$$\mathrm{Rn} = R_O e^{bz} \ldots\ldots\ldots \quad (5)$$

where: 'Rn' is the shale resistivity in the normal compaction states; 'R_0' is the shale resistivity in a mudline; 'b' is the constant while 'Z' is the depth below the mud line.

By substituting the equation (5) into equation (4), Eaton resistivity equations can be written:

$$Ppg = \mathrm{OBG} - (\mathrm{OBG} - \mathrm{Png})\left(\frac{\mathrm{R}}{R_O e^{bz}}\right)^{n} \ldots. \quad (6)$$

where 'R' is the shale resistivity measured at depth 'Z'; Ro is the normal compaction shale resistivity in the mudline and 'b' is the logarithmic resistivity normal compaction line slope; Png is the normal or hydrostatic pressure; OBG is overburden gradient.

2.5. Bower's original method

Compressional velocity was determined in this work using Bower's equation (equation.7)

$$Vp = V0 + A\sigma \mathrm{e}^{B} \ldots\ldots\ldots \quad (7)$$

where *vp* is the compressional velocity at a given depth; *V0* is the compressional velocity in the mudline (i.e., the seafloor or the ground surface, normally *V0l* is approximately 5000 ft/s, or 1520 m/s) so 5000m/s was used; *A* and *B* are the parameters calibrated with offset velocity versus effective stress data, $\sigma \mathrm{e}$ is effective stress.

2.6. Fracture pressure determination

In this work, Matthews and Kelly's [26] method was used for the estimation of fracture pressure (Figure.3.4.). That is fracture pressure (equation 8) gradient is given as

$$FG = k_1 (S - P) + P \ldots\ldots\ldots \quad (8)$$

where S is the overburden stress gradient; *P* is the pore pressure gradient, and $k_1$is the matrix stress or effective stress coefficient.

2.7. Well correlation and seismic section interpretation

The correlated reservoirs were used as the top of sand on the seismic section, which corresponded to a particular amplitude to be mapped. The 3D seismic data of the Cobalt field was provided in SEY format and was loaded onto Petrel 2017 software. Before loading the seismic data on petrel, the project setting was done to carry out coordinate referencing and to set the data to correct units. After loading the data, it was confirmed to be fine through a quality check. The loaded seismic was realized to reduce the volume for easy interpretation or to see the structures well.

The structural interpretation, which consists of fault mapping to get a good understanding of the structural framework of the Cobalt field, was carried out. Structural smoothening was used to enhance the seismic reflections for better interpretations of the faults. The variance attributes (displayed on a time slice) helped in the understanding of the fault trend. This attribute helps increase the clarity of the seismic data for easy and accurate interpretation.

The seismic to well tie was performed using a corrected sonic log and well check shot data. The Checkshot is used to calibrate the relationship between well depths and times calculated from a sonic log. Well tie allows well data, which is in depth, to be compared to seismic data, which is in time. This helps to generate a synthetic seismogram using a Ricker wavelet, which has a good fit and further helps to pick the horizon on the seismic section. The horizons were mapped across the inline and crossline to produce time and depth maps.

The horizons were neatly picked across inline and cross lines, after which they aided in the production of fault polygons. Four horizons were picked, corresponding to the top and base of each reservoir. From the fault polygons, boundaries were generated, which led to the production of time-structural maps.

Time structural maps were generated for the four surfaces from the integration of the fault polygons, boundary polygons, and each horizon. After that, time structure maps were converted using the function to generate depth structural maps to show the distribution of top of overpressures.

3. Results and discussion

From the analysis gotten from well log and seismic data, the overburden stress, the mechanical stratigraphy flag, pore pressure prediction, and fracture pressure together with seismic interpretation are explained in detail.

3.1. Overburden stress

The overburden stress is increasing with an increase in depth. The overburden stress and depth readings all begin with 0 ft, 0 psi, and the overburden stress ranges from a minimum of 0 psi to 111130.1 psi as the maximum, which is in Well one. The table (Table 1) shows the minimum and maximum overburden stress for each well and the minimum depths at which the overburden stress value begins to change from zero psi (0 psi). Overburden stress was found to increase with increasing depths into the subsurface.

Table 1 Minimum and maximum values o overburden stress

Well Name	Depth(ft)	Overburden stress min (psi)	Depth(ft)	Overburden stress max (psi)
Cobalt_01	69.5	0.22	11117.5	11130.1
Cobalt_02	74.5	0.22	12336	1089.02
Cobalt_03	72.5	0.22	12120	11119.50
Cobalt_04	95.5	0.22	10300	8815.95
Cobalt_05	116	0.22	10160	9126.63
Cobalt_06	108	0.22	1167	8898.45

Table 2. Results of pore pressures shows top of overpressure wells for overpressured wells and maximum pressures of each well

Well name	Top of over-pressure(ft)	Start pres-sure(ppg)	Max depth(ft)	Max pressure. (ppg)	State
Cobalt_01		7.73	11117.5	8.61	Normal pressured
Cobalt_02	11140	8.61	1288	10.9	Over pressured
Cobalt_03	11437	8.61	12057	9.5	Over pressured
Cobalt_04	9663.5	8.57	9674	10.5	Over pressured
Cobalt_05	9555	8.55	1019	10.01	Over pressured
Cobalt_06		7.73	1067	8.57	Normal pressured

Table.3. Minimum and maximum fracture pressures

Well Name	Depths(ft)	Minimum fracture pressure(ppg)	Max(ft)	Maximum fracture pressure(ppg)
Cobalt-01	3119	13.27	1081	16.61
Cobalt-02	4585.5	12.27	12307	16.61
Cobalt-03	3441	11.3	12057	15.6
Cobalt-04	4774	12.86	10025	15.01
Cobalt-05	4887	13.50	10144	15.43
Cobalt-06	7606.5	14.08	10778.5	15.06

3.2. Mechanical stratigraphy

The mechanical stratigraphy shale flag is shown below (Figure.3.1a-f) for all the wells, respectively, showing the lithologies for each well. Their results showed that thicker sequences of sand are at shallower depths up to 5000 ft and above are intercalations of sands and shales, up to 9000 ft and above 9000 ft are made of thicker sequences of shales, thin clays, and small pockets of sand. This reflects the stratigraphy of the Niger Delta, where the youngest is the Benin Formation consisting of continental sands and gravel, the Agbada Formation, which is a paralic sequence of interbedded sandstones and shales, and lastly, the Akata Formation, which is predominantly shales and clays with some turbidites and small sand bodies.

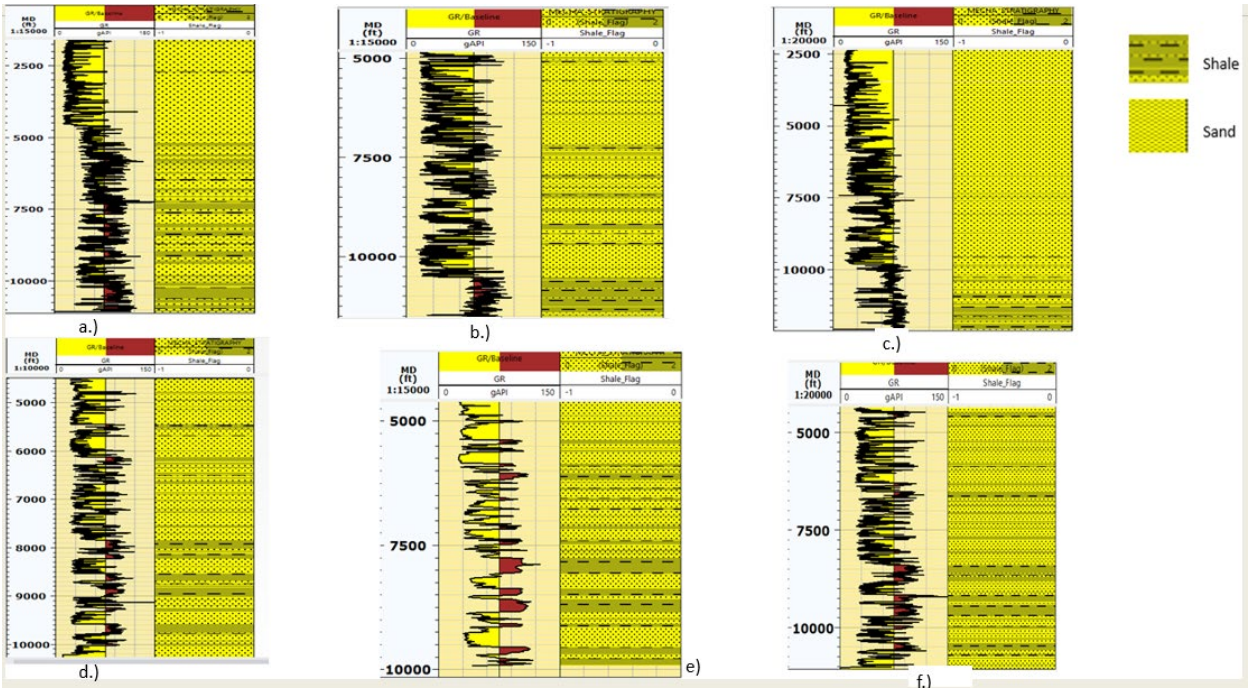

Figure. 3.a-f. Display of lithologies for the six wells respectively

3.3. Pore and fracture pressure prediction

In Cobalt_01 and Cobalt_06, pressure values begin at 7.73ppg and increase with depth, with the normal pressure of 8.61ppg and an Eaton resistivity value of 8.61ppg for Cobalt_01. These pressure values are within the normal pressure of 0.433 psi/ft or 8.5 ppg and wells with predicted pore pressure values are considered normal pressure wells or hydraulically pressured wells. Eaton's Resistivity obtained values for shallow depths were as high as 8.7 ppg but were not considered because the shallow depths contain fresh water and fresh water has high resistivity. The resistivity log is not good to be used alone since the resistivity log is affected by many factors such as salinity, anisotropy, borehole diameter, drilling fluid, lithology, and temperature. Therefore, corrections are needed when these effects are profound. Also, according to [27], pore pressure near the wellbore is affected by the induced stresses and, therefore, deep resistivity is used for calculating pore pressure. The pore pressure within this range of 8.61 ppg shows that this well is a normal pressure (Table 2) as this is illustrated in the line plot (Figure. 4a) and the normal trend is shown in the cross plot (Figure. 4b).

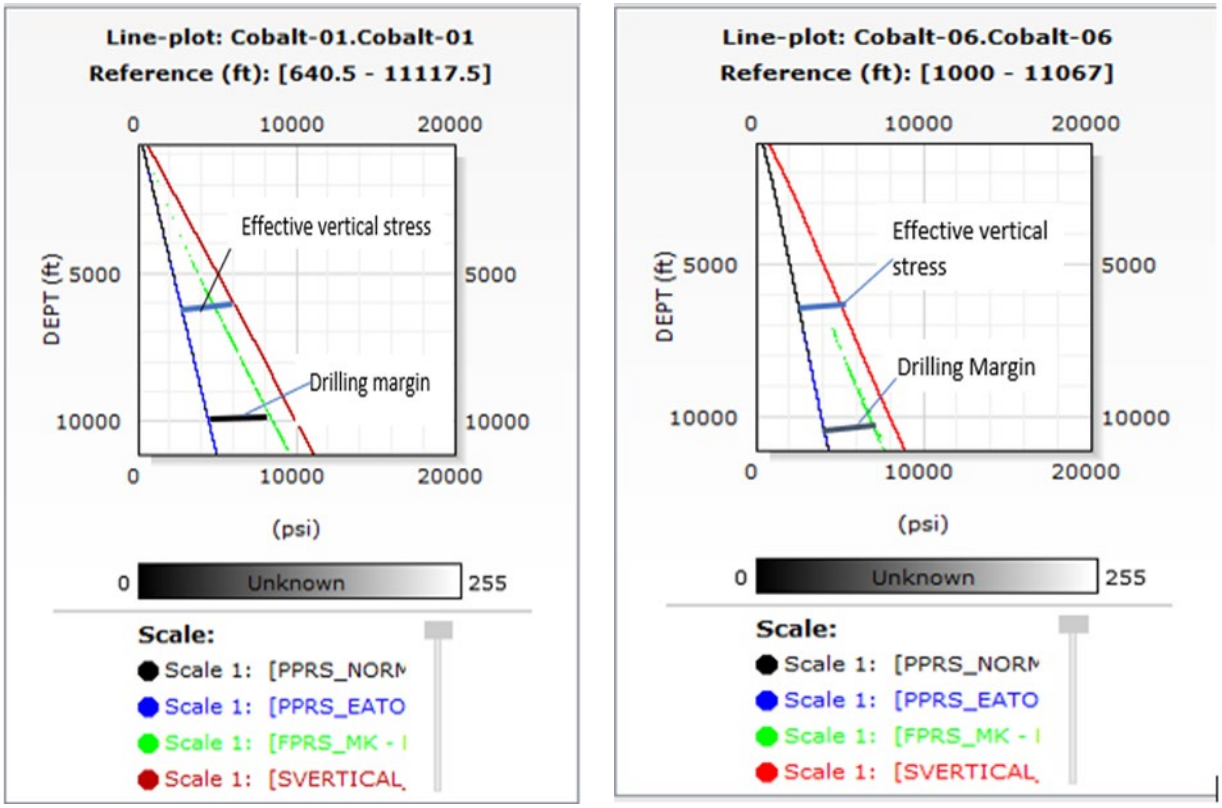

a b

Figure 4 a-b Line plots displaying overburden pressure with Eaton's resistivity pore pressure, normal pressures and fracture pressures with depth showing normal pressure for Cobalt_01 and Cobalt_06 respectively

The fracture pressure ranges from 13.27 ppg at 3119 ft. and 16.61 ppg at 10981 ft. and it is also shown in Table 3. The fracture pressure is normally considered as the upper or maximum bound of the drilling mud weight. If the drilling mud weight exceeds the formation, it will crack and the drilling fluid will get lost into the formation. Information about fracture pressure also important to select the casing design for wells.

Cobalt_06 has the same characteristics as Cobalt_01. The pressure values start at 7.73 ppg and increase hydrostatically up to 11067 ft with a pressure of 8.57 ppg for Eaton resistivity obtained value (Figure. 4b). This pressure is within the normal pressure range which is about 8.5 ppg or 0.433 psi/ft. There is a Sonic log present for this well, but it is not good enough to be used and the sonic log is incomplete as it is difficult to draw a normal compaction trendline.

Pore pressure values including those of Cobalt-06 are presented on Table 2 while those of fracture pressure are presented on Table 3. The fracture pressure values range from 14.08 ppg at 7666.5ft to 15.06 ppg at 10778.5ft. As mentioned earlier, the fracture pressure, which is considered the upper or maximum bound of drilling mud weight. these values will help to design the maximum mud weight and casing setting here. Line plots are displayed (Figures 4a and 4b) to show pressure plots for normally pressured or hydrostatic wells.

Wells with high pressures are shown as the Eaton Resistivity and Eaton Sonic methods together with the Bowers method, are tracking each other and have higher values that are greater than hydrostatic pressure (Cobalt_02, Cobalt_03, and Cobalt_04). While for wells that have only Resistivity log (Eaton's resistivity method), the pore pressure values are high for overpressure wells as seen in Cobalt_05.

In Cobalt_02, the pressure values increase hydrostatically with depth. It starts with normal pressures of 8.52 ppg and pressure values start to increase at the depth of 11140 ft and pressure values of 8.60 ppg (2025.641 psi) (Figure 5a) as the top of overpressure. A maximum pressure value of 10 ppg is reached as shown in Figure (5b) at a depth of 11288.5 ft with pressure values of 9.61 ppg (5633.9psi) for Bowers' original, 10.90 ppg (6423.484psi) for Eaton's Resistivity, and 10.17 ppg (5963.343psi) for Eaton's Sonic, also shown in Table 2.

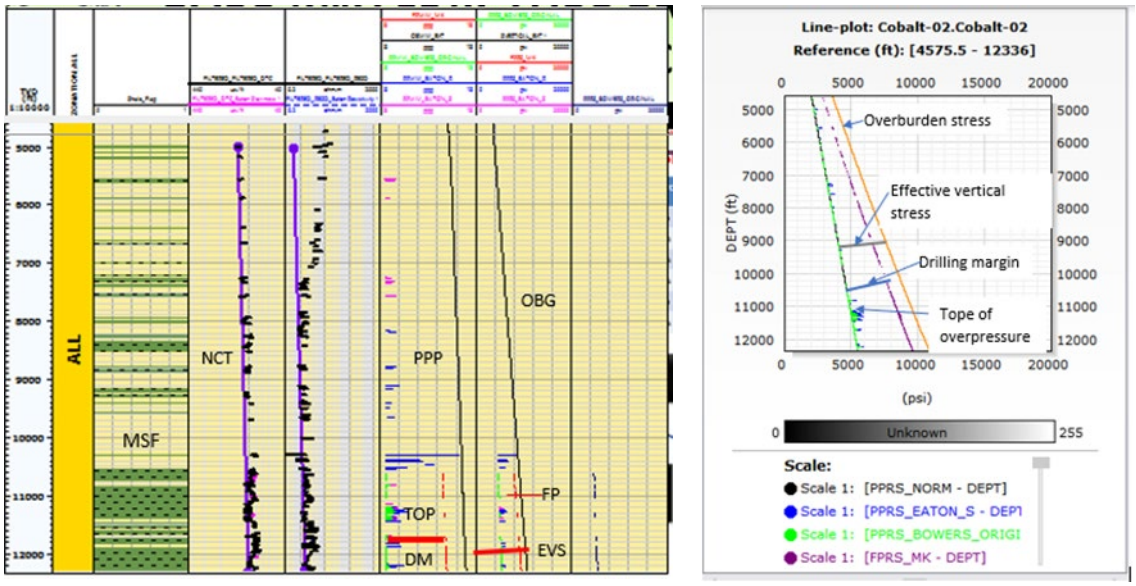

a

Figure 5a shows predicted pore and facture pressure profiles while 5a line plot shows pressure variations with depths and indication top of overpressure and drilling margin

These pressure values are all greater than 8.60 ppg for normal pressure values. Overpressure is observed as the Eaton's sonic and resistivity methods, as well as the Bowers method, track each other. This is seen as a deviation from the normal pressure. The well appears to have been compacting normally up to a depth of 11140 ft and later had some disturbance which led to a deviation from the normal compaction trend. There is a small reduction in bulk density down to 2.15g/cm^3, a reduction of resistivity to 1.37ohms, and a small increment in the sonic log as well, with intercalation of shales and sands. An increase in pore pressure at this depth could be due to fluid expansion as a result of hydrocarbon generation, while further down, as the pore pressure values increase, it is due to an increase in bulk density of up to 2.6g/cm^3 resulting from undercompaction or compaction disequilibrium where sediments compact and the surfaces seal off such that pore fluid cannot be expelled or is expelled at a slower rate. This situation leads to higher pressure values than normal. Figure 5c is a cross plot of derived acoustic velocity (Vp) against Density log which shows the trend representing the different mechanisms causing the overpressure [28]. Cross plot has also been used to show the mechanisms responsible for overpressure in Niger Delta. In addition, the fracture pressure,

which is considered the upper or maximum bound of drilling mud weight for this well. The fracture pressure for this well ranges from 12.27 ppg to 16.61 ppg at 45855 ft to 1230 ft respectively, as presented in Table 3.

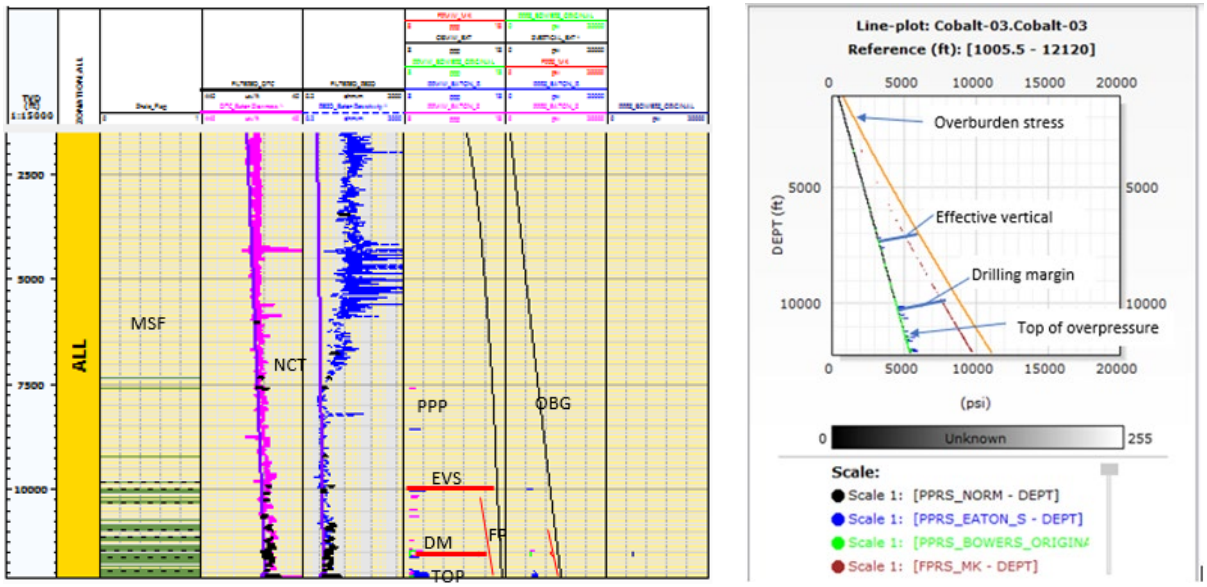

a b

Figure 6a shows predicted pore and facture pressure profiles while 6b line plot shows pressure variations with depths and indication top of overpressure and drilling margin

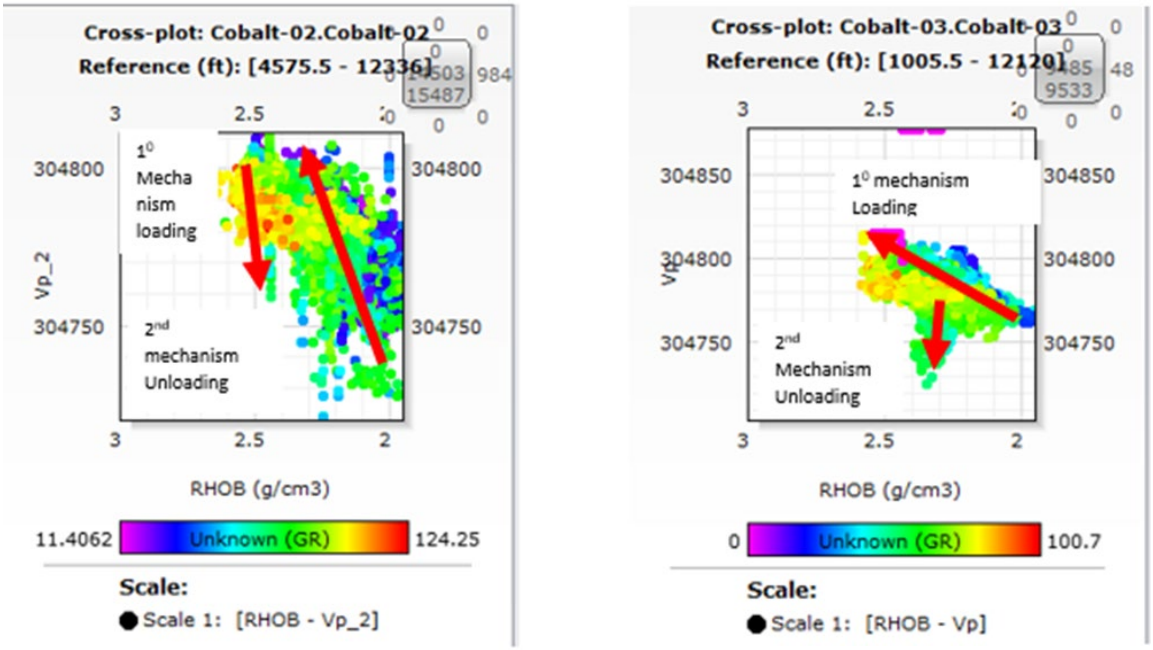

5cc 6c

Figure 5c and 6c. Cross plots showing the trends of different overpressure mechanisms for Well 02 and Well 03 respectively.

Also, Cobalt_03 has similar characteristics as Cobalt_02 and has the same mechanism causing overpressure. In Wells 03, the pressure begins with a normal hydrostatic pressure of 8.4 ppg and the pressure starts increasing at a depth of 11437 ft. This is seen by Eaton Resistivity pressure value of (8.6ppg or 5114.227psi) and Eaton Sonic pressure value (8.6ppg or 5114.227psi) tracking each other together with the Bowers sonic (8.6ppg or 5114.227psi)

method (Figure 6a). The pressure values increase to 9.0 ppg (5618.858 psi), 10.5 ppg (6567.645 psi), and 9.53 ppg (5937.675 psi) at 12025 ft, respectively, and the maximum pressure value is shown in Table 2. This overpressure is indicated on the line plot (Figure 6b) as top of overpressure (11437 ft), which is the depth at which the pressure starts to increase above normal. These pressure values are greater than the values for a normal pressure well. This well is therefore considered an overpressure well as the pressure at this depth deviates from the normal pressure values of 8.5 ppg. Figure 6c shows a cross plot of derived acoustic velocity (vp) against density log, indicating the trends causing the overpressure in Well 03. The fracture pressure for this well ranges from11.3ppg to15.6ppg at 3441ft to 1205ft respectively as shown on Table 3, and is considered as the upper or maximum bound of drilling mud weight for the well.

In Cobalt_04, the pressure also begins with a normal pressure value of 8.47 ppg and an increased pressure as from 9663.5 ft with pressure values of 8.66 ppg (4084.401 psi) for Bowers' original, 8.7 ppg (4109.501) for Eaton's Resistivity, and 9.23(4351.695psi) for Eaton's Sonic, which shows a deviation from the normal hydrostatic pressure (Figure 7a). This is also referred to as the top of overpressure (Figure 7a-b).

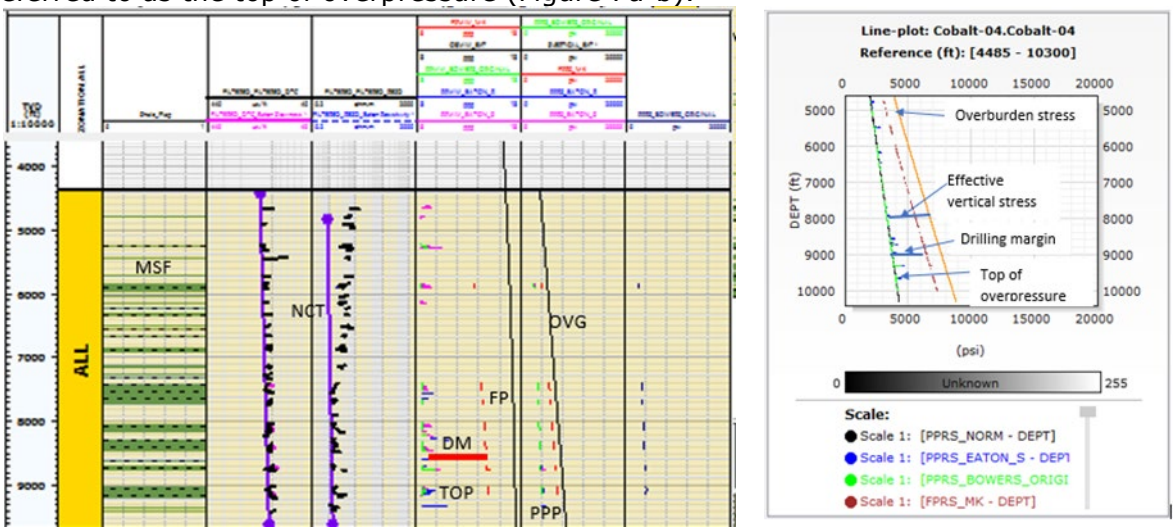

a b

Figure 7a Shows predicted pore and facture pressure profiles while 7b is line plot of pressure variations with depths and indication top of overpressure and drilling margin

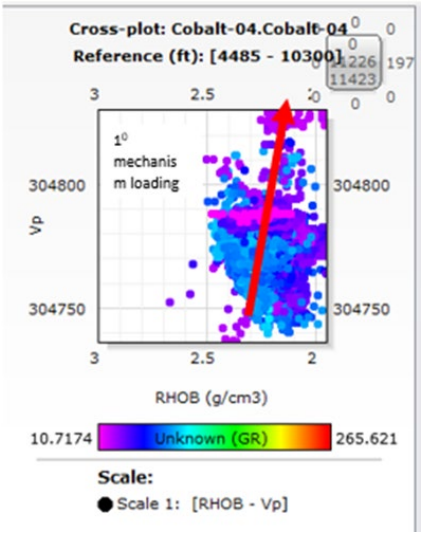

Figure 7c. Cross plots showing the trends of different overpressure mechanisms

The pressure values reach a maximum (Figure 7b) at 9674 ft with pressure values of 8.89 ppg (4201.614psi), 9.94 ppg (4695.166psi) and 9.4 ppg (4470.188psi) respectively for Bowers original, Eaton's Resistivity, and Eaton's Sonic, the highest pressure value is presented in Table 2. The predicted pore pressure for this well is greater than normal pressure values of 8.5 ppg, therefore well 04 is considered overpressured. This increase in pressure is because of the increased density of sediment, which is caused by undercompaction or compaction disequilibrium where there was rapid sedimentation in such a way that the fluid could not be expelled at the faster rate, which eventually led to overpressure. A cross plot of derived acoustic velocity(Vp) against density log (Figure 7c) is used to represent the trend causing overpressure in Cobalt_04.

The fracture pressure for Cobalt_04 ranges from 12.86 ppg at 4774 ft up to 15.43 ppg at a depth of 10025 ft, respectively. The fracture pressure, which is considered the upper or maximum bound of drilling mud weight for this well, shown in Table 3. igure 7a Shows predicted pore and facture pressure profiles while 7b is line plot of pressure variations with depths and indication top of overpressure and drilling margin

In addition, in Cobalt_05, the pressure begins with a pressure that is hydrostatic; that is, pressures of 8.44 ppg, and the pressure increases normally with depth up to 9555 ft with the pressure of 8.61(414.24 psi) for Eaton Resistivity and normal pressure (Figure 8a). It then increases to 10.2 ppg (5075.749 psi) at 10019 ft. The predicted pressure is more than the normal pressure of 8.5 ppg (Figure 8b). This implies that this well is overpressured even though the Sonic log is absent for this well. It would have facilitated the confirmation the pressure values because, as earlier mentioned, the Resistivity log on its own is usually affected by many factors such as hole diameter, fluids, and salinity. It also reads high values for shallow depth as it contains fresh water. This high resistivity at shallow depth is not considered. A cross plot of density log against resistivity log (Figure 8b) shows two trends for the overpressure mechanism, which means that there are two mechanisms that cause overpressure in well 05 (similar Cobalt_02 and Cobalt_03). These are undercompaction and fluid expansion. The fracture pressure for Well 05 ranges from 13.50 ppg at 4887 ft up to 15.43 ppg at a depth of 10144 ft, respectively. The fracture pressure, which is considered as the upper or maximum bound of drilling mud weight for this well, is shown in Table 3.

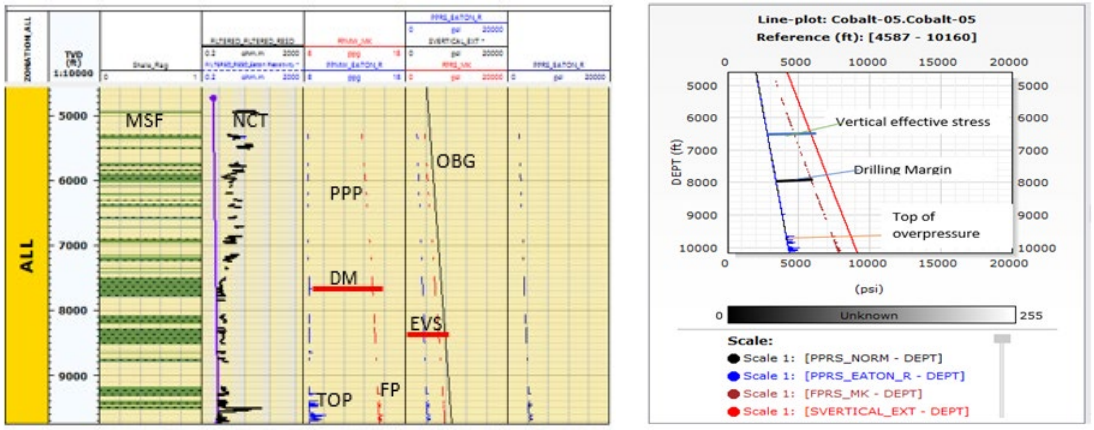

a b

Figure. 8a. Predicted pore pressure profiles, and 8b. Line plot shows pressure variations with depths and indication top of overpressure and drilling margin

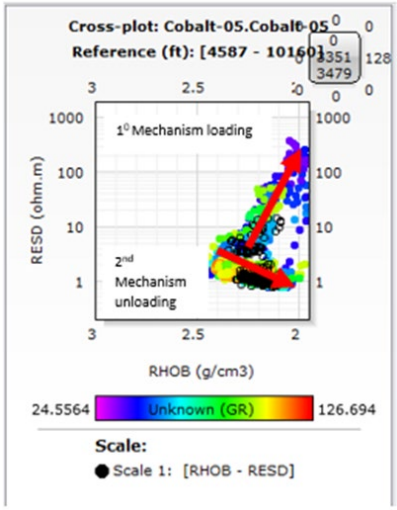

PPRS_NORM: Normal predicted pore pressures
PPRS_EATON_S: Predicted pore pressure using Eaton Sonic Method
PPRS_EATON_R: Predicted pore pressure using Eaton Resistivity Method
FPRS_MK: Predicted fracture pressure using Matthews and Kelly method
SVERTICAL: Overburden stress
PPRS_BOWERS: Predicted pore pressure using Bowers method
1st: Primary
2nd : Secondary
PPP – Predicted pore pressures profiles
OBG- Overburden gradients
NCT: Normal compaction trendline
FP- Fracture pressure
TOP- Top of overpressure
DM- Drilling Margin

Figure 8c. Cross plots showing the trends of different overpressure mechanisms

3.4. Well correlation

Four identified (hydrocarbon bearing) reservoirs were correlated across from the reading of Gamma ray and Resistivity logs. This correlation helps to better access the continuity and lateral extent of the reservoir (Figure 9).

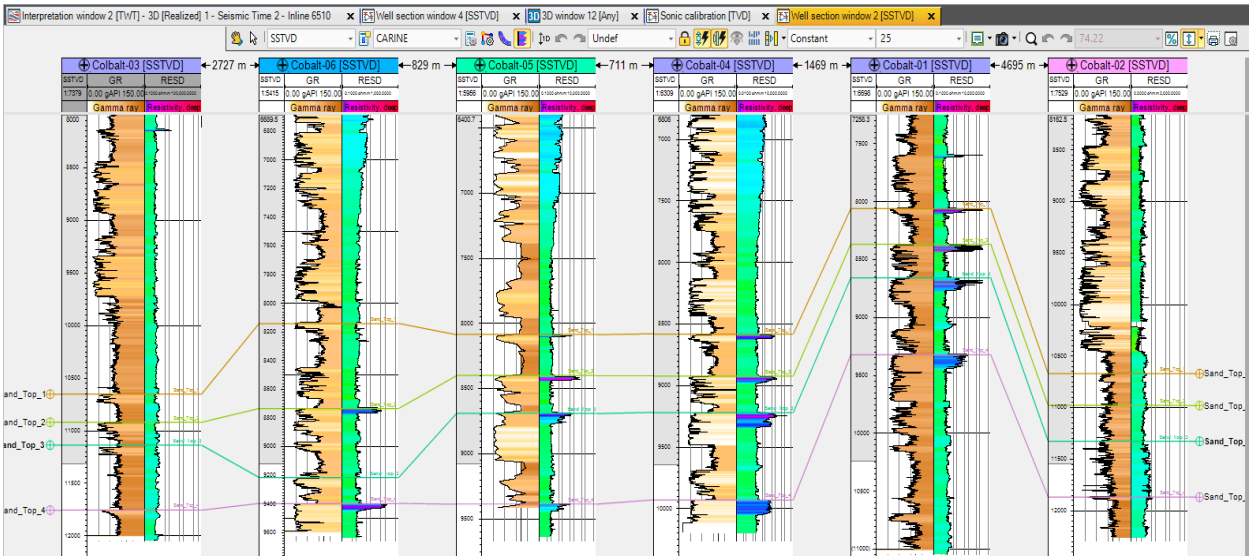

Figure 9. Well correlation section for the wells

3.5. Seismic interpretation

3.5.1. Structural interpretation

Fault mapping was the only structural interpretation carried out in the Cobalt Field. The main structures in the cobalt area are the growth fault and rollover anticline, which could be synthetic or antithetic faults that are listric in nature as the fault flattens with depth, as this is typical of the Niger Delta. The major and minor faults were mapped. This was observed by the abrupt discontinuities in reflection horizons and by the sudden change in the vertical displacement of the reflection horizons. One major fault together with 32 minor faults were picked. It is also observed that the hydrocarbon accumulation is around the rollover anticline, which favors the accumulation [18], as most wells are found between them (Figure 10).

3.5.2. Seismic to well tie

Seismic to well tie was achieved with the help of checkshot data for each well. Here, the wells, which were in depth, were tied to the seismic in time such that the well tops were superimposed on the seismic section (Figure 11). Each reservoir top corresponds to the peaks and troughs on the seismic section as observed from the main reflectors. These tops were mapped as horizons.

3.5.3. Horizon mapping

The horizons were mapped across inline and cross-line and the faults were respected (Figure 10) as it further facilitated the production of subsurface maps.

3.5.4. Time and depths maps, Distribution of top of overpressures

Time maps were generated from the mapped horizons, polygons, and boundaries. These time maps were converted using the plot on (Figure 12) to generate depth maps for each sand unit (Figures 12a, 12b, and 12c) as the wells are penetrating the surfaces, while Figure 13 shows the distribution of all the wells on the combined horizon maps. A majority of the wells are seen to penetrate different fault blocks. The mechanism causing overpressure could be as

a result of lateral transfer from one well to another through the faults. The tops of overpressure wells were found penetrating the different faults (Figure 12d). This shows that the top of overpressured wells is compartmentalized into the different fault blocks (12a-c and Figure 12d).

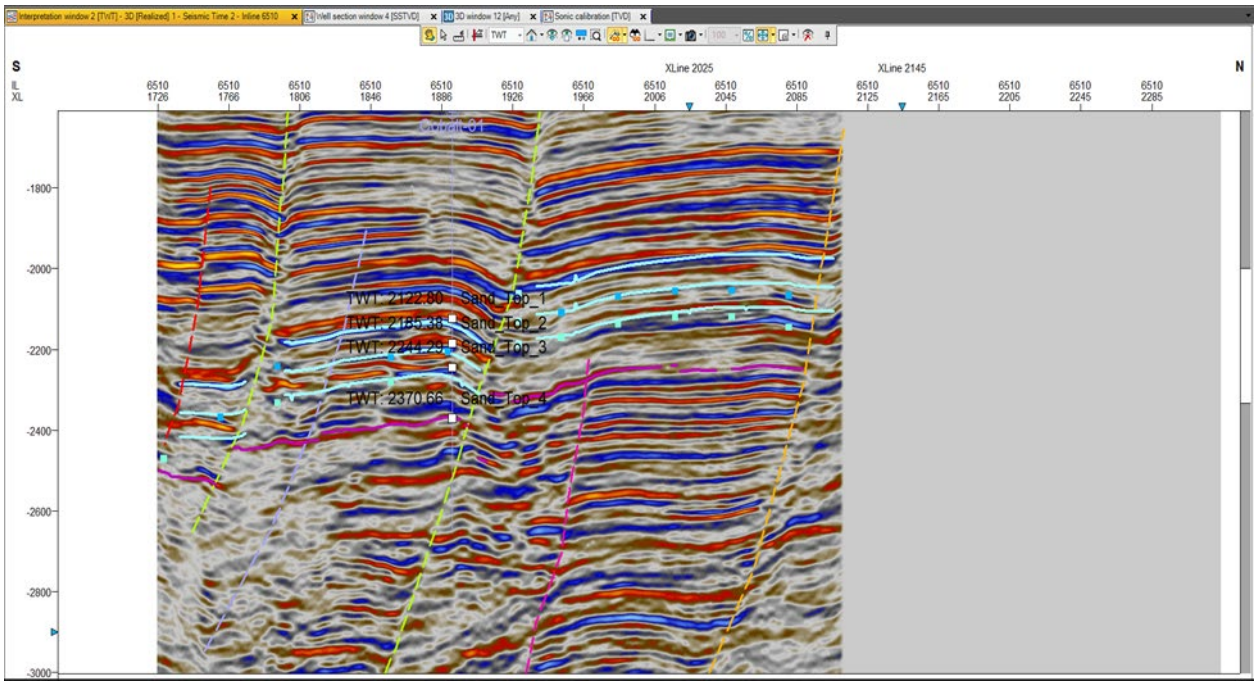

Figure 10. Seismic section showing the mapped faults and sand tops

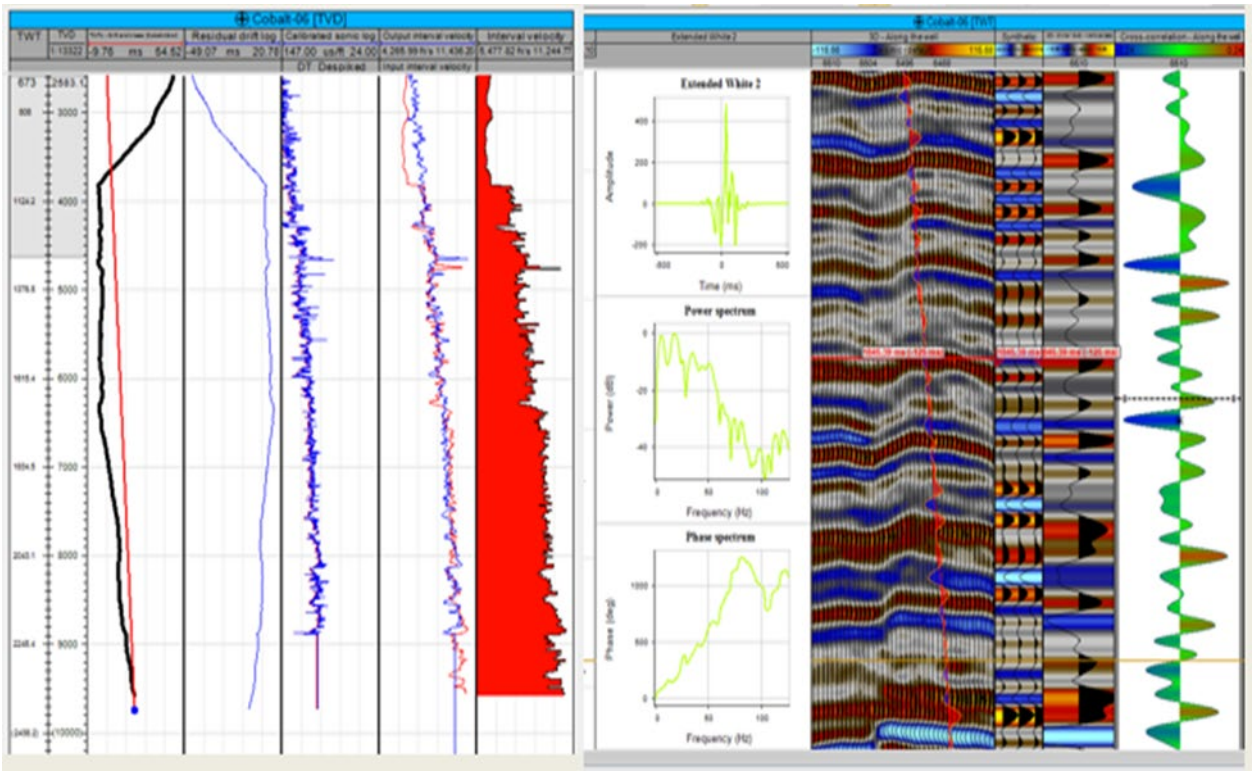

Figure 11. Calibration plate showing synthetic seismogram

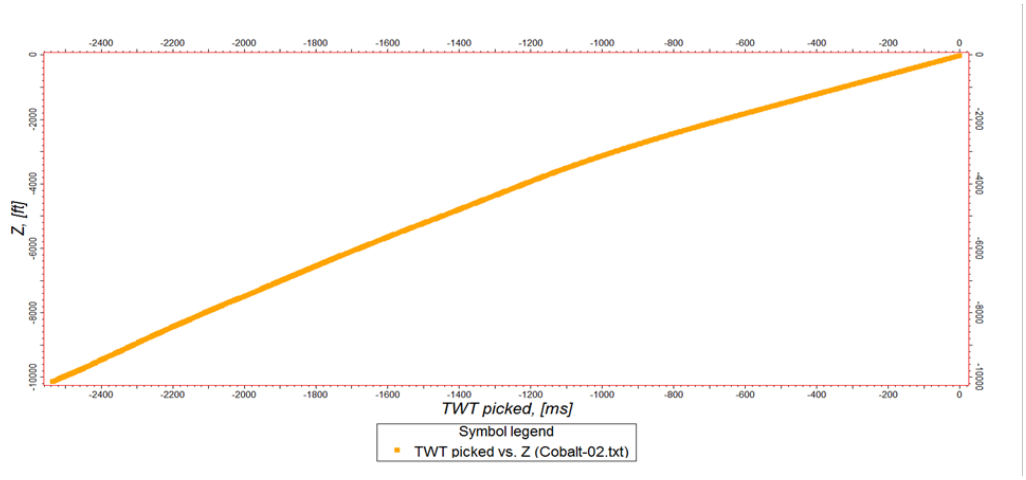

Figure 12. Time - depth relationship used for the conversion of time maps to depth maps

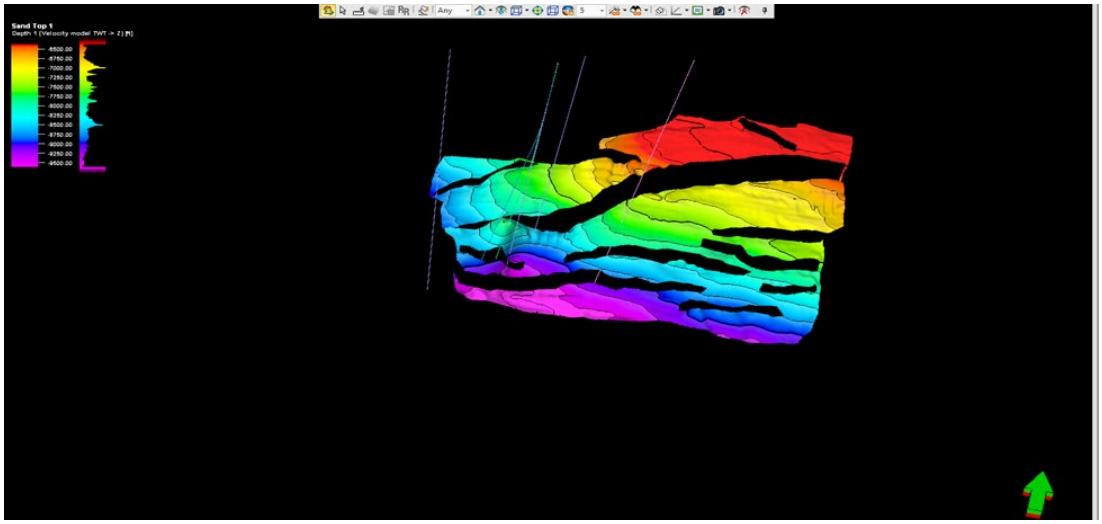

Figure. 12a. Distribution of wells on the depth map for sand top 1

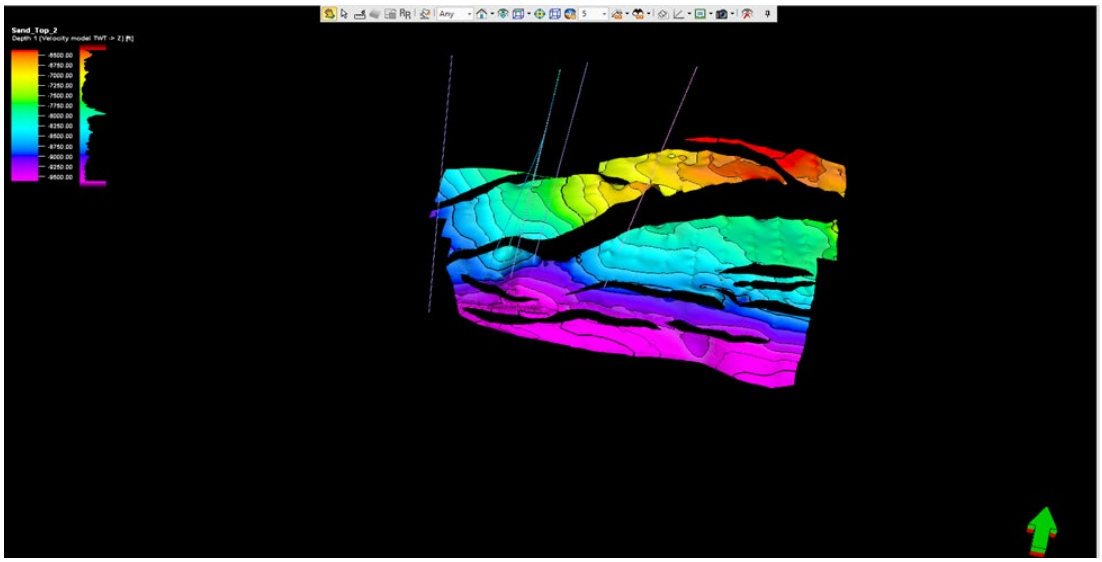

Figure. 12b. Distribution of wells on the depth map for sand top 2

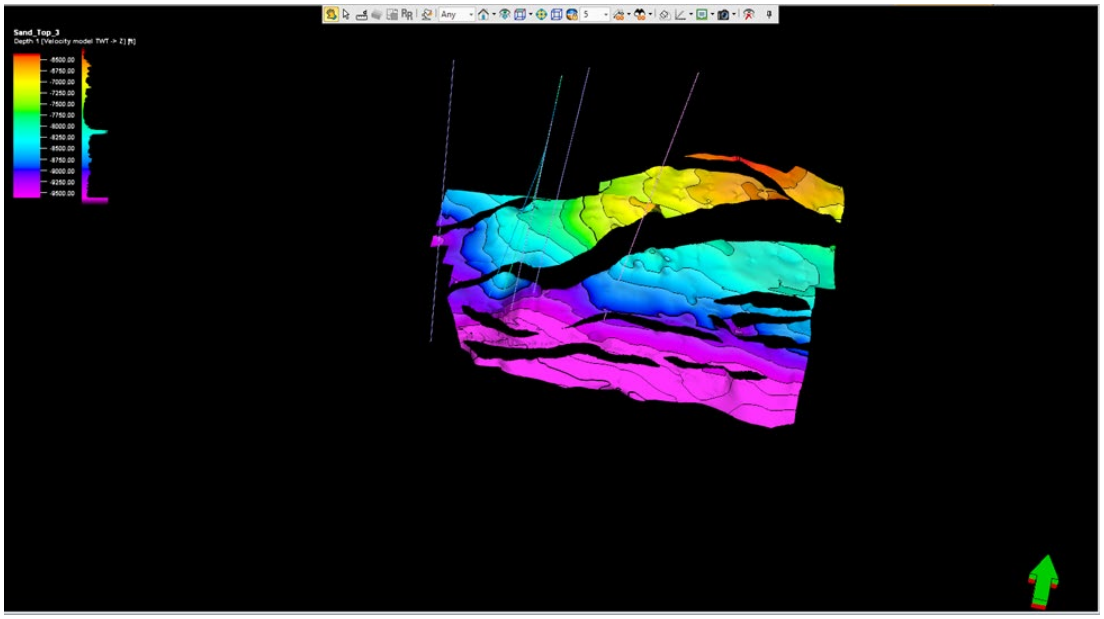

Figure 12c. Distribution of wells on the depth map for sand top 3

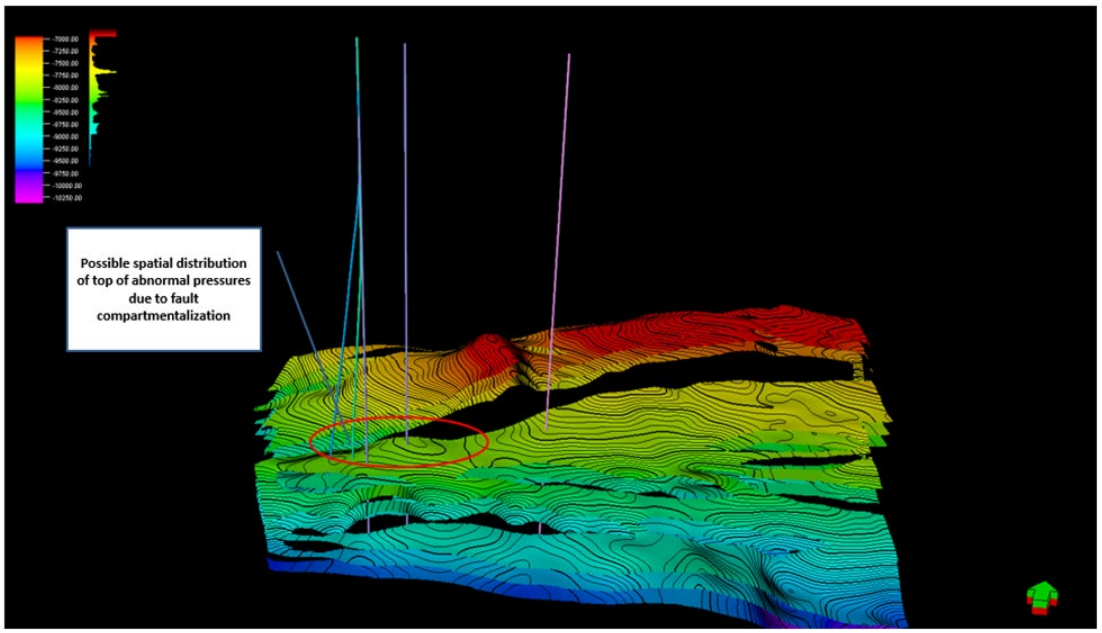

Figure 12d. Distribution of Top of overpressure wells on the top of overpressure map.

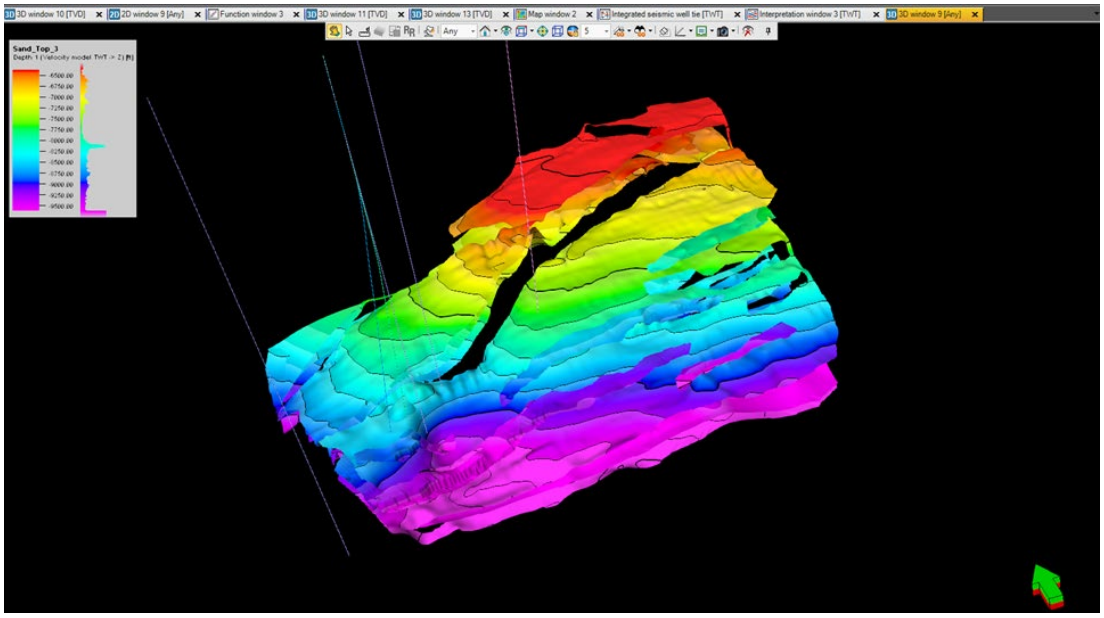

Figure 13 Distribution of all the wells on the combine depth maps

3.6. Implication of predicted pore and fracture pressure on wellbore stability

Pore pressure prediction using Eaton's depth-dependent resistivity and sonic with an applied compaction trendline and Bower's method gave excellent pore pressure prediction. This is because the pore pressures reported in other fields in Niger Delta have proven that overpressure mechanism is a result of disequilibrium compaction(loading) and fluid expansion(unloading) especially being Tertiary Basin [29-33]. From the results obtained for pore pressure prediction and the estimated fracture pressures for each, each well has a minimum and upper bound mud weight that is required to penetrate the formation. The pore pressures predicted for wells 01, 02, 03, 04, 05, and 06 are listed below. The predicted pore pressure gives the drillers the minimum mud weight required to drill the formation. That is, the mud weight should be designed not to be below the predicted pore pressure. If the well is drilled below this pressure, it could lead to well influx, kicks, which if not handled well, would lead to blowouts, and if the well is drilled above the predicted pressure, it could cause sticking of pipes. The predicted fracture pressure is the upper limit or bound for which if the drilling fluid goes above it, it will fracture the formation, and lost circulation will occur. It can also cause the formation to collapse. That is, the fracture pressure also aids in the selection of the casing that would be required to be placed in the well, because the fracture pressure selects the correct casing to fit a specific depth. This prevents the formation from collapsing, damage (cracks), and gives the borehole stability. Figure 6 depicts the workflow for each well as well as the drilling margin.

4. Conclusion

The pore pressure predicted for the six wells in the Cobalt fields shows that four wells were overpressured (Cobalt-02, 03, 04, and 05) while two were normal pressure wells (Cobalt-01 and 06). This means that wells Cobalt-01 and Cobalt-06 will require the drilling mud (fluid) weight to remain between the hydrostatic pressure and not go below or higher than the hydrostatic pressure. For the overpressure wells, Cobalt-02, Cobalt-03, Cobalt-04, and Cobalt-05 the drilling fluid weight should be added to 10.9ppg, 10.5ppg, 9.94ppg, and 10ppg according to the wells respectively to meet these pressure values needed to balance the formation pressure. Their fracture pressures would also help to select the correct casing that will hold the formation to prevent it from instability or lost circulations. Structural interpretation with seismic volume has been able to show the distribution of top of abnormal pressure in the

overpressured wells, hence it can be concluded that these tops of abnormal pressure is compartmentalized within different fault blocks. It can be concluded that, pore and fracture pressures were predicted for COBALT field in Niger Delta Nigeria using well log and seismic data. This information can facilitate proper planning and drilling of future wells in the field.

Acknowledgements

We are grateful to Pan African Union for the financial support to see us through this program for a successful completion. Special thanks go to the staff of Geology Department and for facilitating this study by allowing us to use the Chevron subsurface lab and its resources.

References

[1] Mouchet JP, and Mitchell A. Abnormal Pressure While Drilling. Manuals Techniques 2. Boussens, France. Elf Aquitaine Editions. 1989.
[2] Ayodele Ol, Donker JVB, and Opuwari M. Pore Pressure Prediction of selected wells from the Southern Pletmos Basin, Offshore South Africa. South Africa Journal of Geology. 2016; 119(1): 203-214.
[3] Opara LA, and Onuoha MK. Predrill Pore Pressure Prediction 3-D Seismic Data in Parts of the Onshore Niger Delta Basin SOC. Proceedings of Nigeria Annual International Conference and Exhibition, (NAICE'09). 2009.
[4] Flemming PB, and Lupa JA. Pressure prediction in the Bullwinkle Basin through petrophysics and flow modeling (green Canyon 65, Gulf of Mexico) Mar. Pet. Geol. 2004; 1311-132, p. 21.
[5] Gaarenstroom L, Tromp RAJ, Jong MD, and Brandenburg A. Overpressures in the Central North Sea: Implications for Trap Integrity and Drilling Safety, Petroleum Geology Conference Series. Geological Society of London. 2005; 4(1):1305-1313.
[6] Hunt JM. Generation and migration of petroleum from abnormally pressured fluid compartments (1) AAPG Bull. 1990; 74: 1-12.
[7] Chopra S, and Huffman A. Velocity determination for pore pressure prediction. CSEG Rec, 2006; 31(4): 25: 29–46.
[8] Iliffe J, Robertson A, Ward G, Wynn C, Pead S, and Cameron N. The Importance of Fluid Pressures and Migration to the Hydrocarbon Prospectivity of the Faeroe–Shetland White Zone, Petroleum Geology Conference Series. Geological Society of London. 1999; 601-611.
[9] Hottmann CE, and Johnson RK. Estimation of Formation Pressures from Log Derived Shale Properties. References Scientific Research Publishing, Journal of Petroleum Technology. 1965; 17: 717-722.
[10] Fertl WH, Chilingarian GV. Abnormal Formation Pressures and Their Detection by Pulsed Neutron Capture Logs Journal of Petroleum Science and Engineering. 1987; 1: 23 – 38.
[11] Serebryakov VA, Chilinger GY, and Katz SA. Methods of estimating and predicting abnormal formation pressures. Journal of Petroleum science and Engineering. 1995; 13: 113-123.
[12] Shaker S. Calibration of geopressured prediction using the normal compaction trend: perception and pitfall: CSEG Recorder. 2007; 32(1): 29-35.
[13] Qays MS, Wan IWY. Pore Pressure Prediction and Modeling Using Well-Logging Data in Bai Hassan Oil Field Northern Iraq. Journal of Earth Science & Climatic Change. 2015; 06(07). https://doi.org/10.4172/2157-7617.1000290.
[14] Eaton BA. The Effect of Overburden Stress on Geopressure Prediction from Well Logs SPE 3rd Symposium on Abnormal Pore Pressure, 1972; SPE paper #3719.
[15] Bowers GL. Pore pressure estimation from velocity data: Accounting for overpressure mechanisms besides undercompaction: SPE Drilling and Completions, 1995; 10(2).
[16] Swarbrick RE. Pore pressure prediction: Pitfalls in Using Porosity" OTC Offshore Technology Conference. 2001; https://doi.org/10.4043/13045-MS.
[17] Holland P. Loss of well control occurrence and size Estimators, Phase 1 and 2. ExproSoft AS, Trondheim, 2017; Report no. Version Date ES201471/2.
[18] Doust H, and Omatsola E. Niger Delta, in, Edwards, J.D and Santogrossi, P.A, Divergent/passive Margin Basins, American Association of Petroleum Geologists Memoir. 1990; 48(1): 239-248.
[19] Kulke H. Regional Petroleum Geology of the world. A part II: Africa, Australia and Antactica: Berlin, Gebruder Bogrntraeger. 1995; 143-172.
[20] Hospers J. Gravity field and structure of the Niger Delta, Nigeria, West Africa: Geological Society of American Bulletin. 1965; 76: 407-422.

[21] Short KC, and Stauble AJ. Outline of geology of Niger Delta. American Association of Petroleum Geologists Bulletin. 1965; 51: 761–779.
[22] Avbovbo AA. Tertiary lithostratigraphy of Niger Delta. American Association of Petroleum Geologists, Bulletin 1978; 62: 295-300.
[23] Gibson RE. The progress of consolidation in a clay layer increasing in thickness with time, Geotechnique, 1958; 8: 171-182.
[24] Bredehoeft JD. and Hanshaw BB. On the maintenance of anomalous fluid pressures: I. Thick sedimentary sequences., Geological Society of America Bulletin. 1968; 79: 1097-1106.
[25] Smith JE. Dynamics of shale compaction and evolution of pore-fluid pressure, Mathematical Geol. 1971; 3: 239-263.
[26] Matthews WR. and Kelly J. How to predict formation pressure and fracture gradient Oil Gas J. 1967; 65(8): 92–106.
[27] Zhang J, and Roegiers J.-C. Double porosity finite element method for borehole modeling Rock Mech. Rock Engng. 2005; 38: 217–242 .
[28] Nwankwo CN, and Kalu SO. Integrated Approach to Pore Pressure and Fracture Pressure Prediction Using Well Logs: Case Study of Onshore Niger-Delta Sedimentary Basin. Open Journal of Geology. 2016; 6, 1279-1295.
[29] Iftikhar AS, Ddeva G, Wan IWY, and Jamaal H. Origin of Overpressure in a Field in the Southwestern Malay Basin. Proceedings of the Annual Offshore Technology Conference 1 2015; Vol 1. DOI: 10.2118/24736-MS.
[30] Weber KJ. Sedimentological aspects of oil fields in the Niger Delta; Geologic en Mijirobourne. 1971; 50: 559-576.
[31] Evamy BD, Harembourne J, Kamerling P, Knaap WA, Molley FA, and Rowlands PH. Hydrocarbon habitat of the Tertiary Niger Delta; AAPG Bulletin. 1978; 62: 1 –39.
[32] Chapman RE. Mechanical versus thermal cause of abnormal high pore pressure in shales; AAPG Bulletin. 1980; 64: 2179 – 2183.
[33] Hunt JM. Petroleum geochemistry and geology; Freeman Press, San Francisco, USA. 1979; p. 617.
[34] Ehinola OA, Oluwakunle MO, and Olumide EO. Wireline, MWD and Mudlogs: A Three Way Complementary Approach to Reduce Uncertainties in Pore Pressure Analysis in SMK Field, Onshore Niger Delta. Petroleum and Coal. 2017; 59(1): 69-81.

To whom correspondence should be addressed: Mpara Carine Bongka, Pan African University of Life and Earth sciences, Department of Geology, University of Ibadan, Ibadan, Nigeria; e-mail: mpara.carine@gmail.com